

The Effect of Adsorption on the Face Development of the Equilibrium Form

By P. HARTMAN

Kristallografisch Instituut, Rijksuniversiteit, Melkweg 1, Groningen, Netherlands

(Received 3 November 1958)

The effect of adsorption on the zonal development of the equilibrium form is discussed. The surface energy of a face ($hk0$) on which foreign particles are adsorbed is expressed in terms of the surface energies of the two most densely packed faces (100) and (010) and the interaction energies of the adsorbed particles with the crystal chains parallel to [001].

For non-ionic crystals it is found that the face (110) is fairly enhanced if the adsorption takes place at the step edges only. If the adsorption takes place on the whole surface, its effect on the equilibrium form is slight.

For ionic crystals the effects are larger and several examples are studied. To this end approximate formulas are derived for the interaction energy of various types of ionic chains. It was found that adsorption can lead to an abnormal face development of the zone, so that faces with relatively high indices become rather persistent. The high index forms studied include {532} of zircon, {017} and {3,2,19} of anatase, {123}, {124}, {137} and {3,5,11} of fluorite. These faces are all parallel to the direction in which the interaction energy of the crystal ionic chains is zero. A tentative explanation of this effect is given. For zircon and anatase possible sites for adsorbed foreign ions are found.

Introduction

In a previous paper (Hartman, 1958) the face development of a zone was studied under the conditions of thermodynamic equilibrium. It was concluded that, apart from F faces, also S faces may be found on the equilibrium form, especially with non-ionic crystals. For ionic crystals it was found that S forms are not likely to be present on the equilibrium form. Yet many ionic crystals do exhibit S faces. In so far as the occurrence of S faces cannot be explained by the magnitude of the surface energy, there must be other, non-structural factors.

In this paper one of these external factors, namely the adsorption of foreign matter, will be considered. Particularly the anomalous face development of ionic crystals will be discussed and some examples will be treated.

The effect of adsorption on the surface energies

Consider a zone [001] in which two F faces are given the indices (100) and (010). The S_1 face between (100) and (010) be (110). The surface free energy per mesh area of (110) can be written in terms of the same quantities for (100) and (010) plus a correction term:

$$A_{110}\sigma_{110} = A_{100}\sigma_{100} + A_{010}\sigma_{010} + A_{110}\Delta\sigma_{110}. \quad (1)$$

In this equation σ stands for the specific surface free energy of a face and A for its mesh area. It has been shown (Hartman, 1958) that at 0 °K. the correction term $A_{110}\Delta\sigma_{110}$ can be expressed in terms of the interaction energies of the chains parallel to the zone axis [001]:

$$2A_{110}\Delta\sigma_{110} = \sum_{u=-\infty}^{+\infty} \sum_{v=-\infty}^{+\infty} c_{uv}E(u, v). \quad (2)$$

Here $E(u, v)$ is the interaction energy between chains a distance $\mathbf{r}(u, v) = u\mathbf{a}' + v\mathbf{b}'$ apart, where $a' = a \sin \beta$ and $b' = b \sin \alpha$; a, b, α and β being lattice parameters. For each pair of (u, v) values the coefficient c_{uv} is given in the former paper (Hartman, 1958).

Suppose that some impurity particles (atoms, molecules or ions that do not belong to the constituents of the crystal) are adsorbed on ($hk0$). When the specific surface energy of a face after adsorption took place, is denoted by σ' , we can write:

$$A_{hk0}\sigma'_{hk0} = A_{hk0}\sigma_{hk0} + E_a(hk0) \quad (3)$$

where $E_a(hk0)$ represents the adsorption energy per mesh area. When this energy is negative, the surface energy is lowered by adsorption and the face is enhanced.

Equation (1) changes into:

$$A_{110}\sigma'_{110} = A_{100}\sigma'_{100} + A_{010}\sigma'_{010} + A_{110}\sigma'_{110} \quad (4)$$

and the new correction term becomes:

$$A_{110}\Delta\sigma'_{110} = A_{110}\Delta\sigma_{110} + E_a(110) - E_a(100) - E_a(010). \quad (5)$$

Similarly:

$$A_{210}\Delta\sigma'_{210} = A_{210}\Delta\sigma_{210} + E_a(210) - E_a(110) - E_a(100). \quad (6)$$

$$A_{310}\Delta\sigma'_{310} = A_{310}\Delta\sigma_{310} + E_a(310) - E_a(210) - E_a(100). \quad (7)$$

$$A_{320}\Delta\sigma'_{320} = A_{320}\Delta\sigma_{320} + E_a(320) - E_a(210) - E_a(110). \quad (8)$$

Each quantity $E_a(hk0)$ can be expressed in terms of interaction energies between the adsorbed particles

and the chains parallel to $[001]$ of the crystal. We divide the adsorption sites to this end in five types.

Type 1: sites, where particles are adsorbed on (100) only.

Type 2: sites, where particles are adsorbed on (010) only.

Type 3: sites, where particles are adsorbed on that part of a (110) step that is parallel to (100).

Type 4: sites, where particles are adsorbed on that part of a (110) step that is parallel to (010).

Type 5: sites, where particles are adsorbed at the step edge of (110).

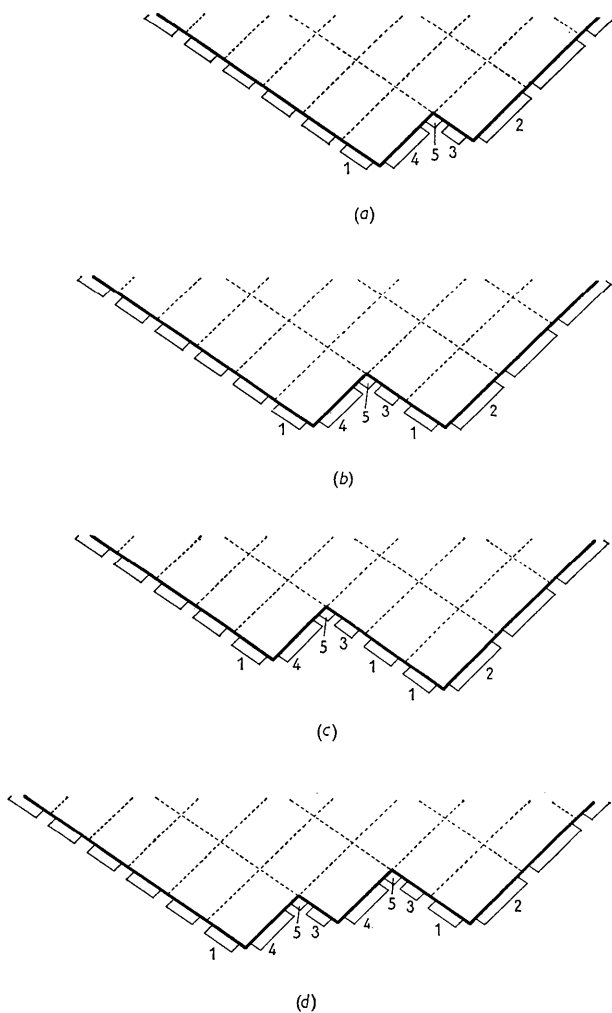


Fig. 1. Profiles of the faces (100), (010) and $(hk0)$, viewed along $[001]$ with various types of sites for adsorbed particles. The $(hk0)$ face is in (a) (110), in (b) (210), in (c) (310) and in (d) (320).

In Fig. 1 these types are indicated on the profiles of various S faces. The profiles of S faces other than (110) can be considered to consist of alternating profile periods of (110) and of (100) or of (010), so

that the five types of adsorption sites are sufficient to describe the effect of adsorption on the zone development. The adsorption energy $E_a(hk0)$ can now be found by adding together the interaction energies of all particles adsorbed on the face with all chains of the crystal. To keep the notation clear, we denote by $\alpha_i E_{ai}(u, v)$ (cf. equation (2)) the interaction energy

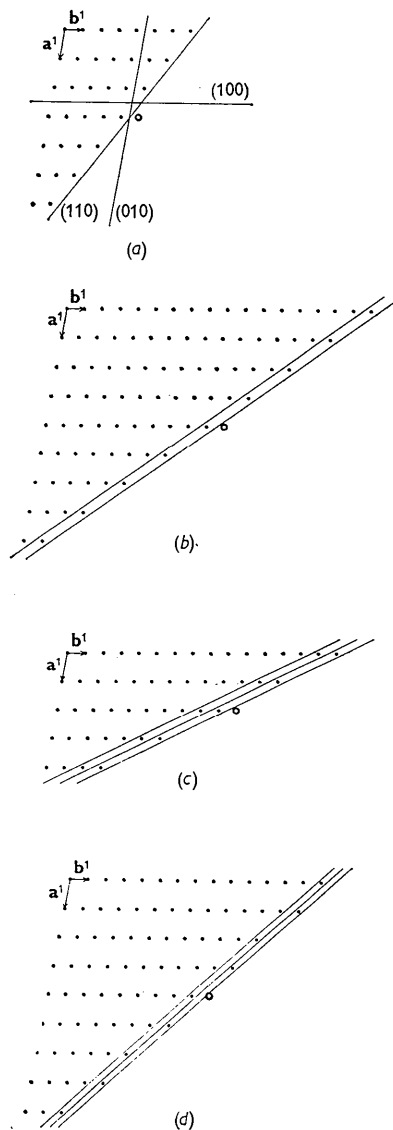


Fig. 2. Crystal boundaries for various adsorption sites. Each dot represents a chain of crystal particles parallel to $[001]$. The circlet represents an adsorbed particle. (a) boundary of (110); (b) boundaries of (210). The boundary nearer to the adsorbed particle corresponds to adsorption sites of types 3, 4 and 5; the other to adsorption sites of type 1; (c) boundaries of (310). The middle and higher boundaries correspond each to a site of type 1; the lower corresponds to sites of types 3, 4 and 5; (d) boundaries of (320). The boundary most remote from the adsorbed particle corresponds to a site of type 1; the other boundaries correspond each to sites of types 3, 4 and 5.

of particles in sites of type i with a certain chain; α_i is the number of these particles per mesh area and the origin is taken in the centre of the chain that would replace the adsorbed material if ordinary growth of the crystal proceeded.

In Fig. 2 this origin is chosen in a fixed chain (outside the crystal of course) and for the various sites of adsorbed particles the boundary of the crystal is drawn.

For (100) we have to consider particles in type 1 sites

$$E_a(100) = \sum_{u=-\infty}^{-1} \sum_{v=-\infty}^{+\infty} \alpha_1 E_{a1}(u, v). \quad (9)$$

For (010) only particles in type 2 sites are possible:

$$E_a(010) = \sum_{u=-\infty}^{+\infty} \sum_{v=-\infty}^{-1} \alpha_2 E_{a2}(u, v). \quad (10)$$

For (110) particles in sites of types 3, 4 and 5 must be considered; for all these types the origin is the same. If we put $m = u+v$, we find:

$$E_a(110) = \sum_{u=-\infty}^{+\infty} \sum_{m=-\infty}^{-1} [\alpha_3 E_{a3}(u, m-u) + \alpha_4 E_{a4}(u, m-u) + \alpha_5 E_{a5}(u, m-u)]. \quad (11)$$

For (210) type 1 sites have a different origin than sites of types 3, 4 and 5. If we put $p = 2u+v$, we find:

$$E_a(210) = \sum_{u=-\infty}^{+\infty} \sum_{p=-\infty}^{-2} \alpha_1 E_{a1}(u, p-2u) + \sum_{u=-\infty}^{+\infty} \sum_{p=-\infty}^{-1} [\alpha_3 E_{a3}(u, p-2u) + \alpha_4 E_{a4}(u, p-2u) + \alpha_5 E_{a5}(u, p-2u)]. \quad (12)$$

For (310) three different origins and therefore three different crystal boundaries have to be considered. If we put $q = 3u+v$, we find:

$$E_a(310) = \sum_{u=-\infty}^{+\infty} \sum_{q=-\infty}^{-3} \alpha_1 E_{a1}(u, q-3u) + \sum_{u=-\infty}^{+\infty} \sum_{q=-\infty}^{-2} \alpha_1 E_{a1}(u, q-3u) + \sum_{u=-\infty}^{+\infty} \sum_{q=-\infty}^{-1} [\alpha_3 E_{a3}(u, q-3u) + \alpha_4 E_{a4}(u, q-3u) + \alpha_5 E_{a5}(u, q-3u)]. \quad (13)$$

For (320) we also find three different boundaries. Putting $s = 3u+2v$ and $m = u+v$, we find:

$$E_a(320) = \sum_{m=-\infty}^{+\infty} \sum_{s=-\infty}^{-3} \alpha_1 E_{a1}(s-2m, 3m-s) + \sum_{m=-\infty}^{+\infty} \sum_{s=-\infty}^{-2} [\alpha_3 E_{a3}(s-2m, 3m-s) + \alpha_4 E_{a4}(s-2m, 3m-s) + \alpha_5 E_{a5}(s-2m, 3m-s)] + \sum_{m=-\infty}^{+\infty} \sum_{s=-\infty}^{-1} [\alpha_3 E_{a3}(s-2m, 3m-s) + \alpha_4 E_{a4}(s-2m, 3m-s) + \alpha_5 E_{a5}(s-2m, 3m-s)]. \quad (14)$$

The substitution of (9) to (14) into (5) to (8) gives us the desired correction term for the surface energy. In this general form the result is rather complicated. We will examine the zonal development for some simple extreme cases of adsorption.

Zonal development of non-ionic crystals with adsorption

Case 1

The first case to be studied is the adsorption of many particles per mesh area. We suppose that the interaction energy is restricted to chains with the following values of (u, v) : $(1, \bar{1})$, $(0, \bar{1})$, $(\bar{1}, \bar{1})$, $(\bar{1}, 0)$ and $(\bar{1}, 1)$. Furthermore we suppose that:

- (1) The adsorption layer is only one molecule thick.
- (2) The mesh areas are relatively large compared to the adsorbed particles, so that α_5 is negligibly small, while $\alpha_3 = \alpha_1$ and $\alpha_4 = \alpha_2$.

This occurs e.g. when a crystal is surrounded by its saturated solution or when its vapour contains foreign gases.

As a consequence the difference between type 1 and type 3 sites has disappeared and so has the difference between type 2 and type 4 sites. Hence we put:

$$E_{a1}(u, v) = E_{a3}(u, v) \text{ and } E_{a2}(u, v) = E_{a4}(u, v).$$

We find then:

$$A_{110} \Delta \sigma'_{110} = A_{110} \Delta \sigma_{110} + \alpha_1 [E_{a1}(0, \bar{1}) - E_{a1}(\bar{1}, 1)] + \alpha_2 [E_{a2}(\bar{1}, 0) - E_{a2}(1, \bar{1})].$$

$$A_{210} \Delta \sigma'_{210} = A_{210} \Delta \sigma_{210} + \alpha_2 E_{a2}(\bar{1}, 1).$$

$$A_{310} \Delta \sigma'_{310} = A_{310} \Delta \sigma_{310} \text{ and } A_{320} \Delta \sigma'_{320} = A_{320} \Delta \sigma_{320}.$$

Because

$$|E_{a1}(0, \bar{1})| > |E_{a1}(\bar{1}, 1)| \text{ and } |E_{a2}(\bar{1}, 0)| > |E_{a2}(1, \bar{1})|$$

the face (110) is enhanced. The face (210) is but slightly enhanced, while all other faces retain their areas.

Case 2

Again we consider an adsorption on all kinds of faces, but this time it is supposed that the mesh areas are of the same order of magnitude as the adsorbed particles so that type 3 and type 4 do not occur. Then $E_{a1}(u, v) = E_{a2}(u, v) = E_{a5}(u, v) = E_a(u, v)$ and we obtain:

$$\begin{aligned} A_{110}\Delta\sigma'_{110} &= A_{110}\Delta\sigma_{110} - (\alpha_1 + \alpha_2 - \alpha_5)E_a(\bar{1}, \bar{1}) \\ &\quad - (\alpha_1 - \alpha_5)E_a(\bar{1}, 0) - (\alpha_2 - \alpha_5)E_a(0, \bar{1}) \\ &\quad - \alpha_1 E_a(\bar{1}, 1) - \alpha_2 E_a(1, \bar{1}). \\ A_{210}\Delta\sigma'_{210} &= A_{210}\Delta\sigma_{210} + (\alpha_5 - \alpha_1)E_a(\bar{1}, 1). \end{aligned}$$

If we suppose that $\alpha_1 = \alpha_2 = \alpha_5$ (this presumably occurs when the foreign particles are solvent molecules) the face (110) will be slightly diminished, while the areas of the other S faces do not change.

If, on the other hand, we suppose that $\alpha_5 \gg \alpha_1$ and $\alpha_5 \gg \alpha_2$ the face (110) is enhanced, and so is (210), though not so much.

Case 3

The adsorption takes place exclusively at the step edges, so that only particles in sites of type 5 are present. In view of the following treatment of ionic crystals we take into account all interaction energies $E_{a5}(u, v)$ and we drop the subscript 5. We find:

$$A_{110}\Delta\sigma'_{110} = A_{110}\Delta\sigma_{110} + \sum_{u=-\infty}^{+\infty} \sum_{m=-\infty}^{-1} \alpha E_a(u, m-u). \quad (15)$$

$$\begin{aligned} A_{210}\Delta\sigma'_{210} &= A_{210}\Delta\sigma_{210} + \sum_{u=-\infty}^{+\infty} \sum_{p=-\infty}^{-1} \alpha E_a(u, p-2u) \\ &\quad - \sum_{u=-\infty}^{+\infty} \sum_{m=-\infty}^{-1} \alpha E_a(u, m-u) \\ &= A_{210}\Delta\sigma_{210} + \sum_{m=0}^{+\infty} \sum_{p=-\infty}^{-1} \alpha E_a(p-m, 2m-p) \\ &\quad - \sum_{m=-\infty}^{-1} \sum_{p=0}^{+\infty} \alpha E_a(p-m, 2m-p) \end{aligned} \quad (16)$$

$$\begin{aligned} A_{310}\Delta\sigma'_{310} &= A_{310}\Delta\sigma_{310} + \sum_{u=-\infty}^{+\infty} \sum_{q=-\infty}^{-1} \alpha E_a(u, q-3u) \\ &\quad - \sum_{u=-\infty}^{+\infty} \sum_{p=-\infty}^{-1} \alpha E_a(u, p-2u) \\ &= A_{310}\Delta\sigma_{310} + \sum_{p=0}^{+\infty} \sum_{q=-\infty}^{-1} \alpha E_a(q-p, 3p-2q) \\ &\quad - \sum_{p=-\infty}^{-1} \sum_{q=0}^{+\infty} \alpha E_a(q-p, 3p-2q). \end{aligned} \quad (17)$$

$$\begin{aligned} A_{320}\Delta\sigma'_{320} &= A_{320}\Delta\sigma_{320} + \sum_{m=-\infty}^{+\infty} \sum_{s=-\infty}^{-2} \alpha E_a(s-2m, 3m-s) \\ &\quad + \sum_{m=-\infty}^{+\infty} \sum_{s=-\infty}^{-1} \alpha E_a(s-2m, 3m-s) \\ &\quad - \sum_{u=-\infty}^{+\infty} \sum_{p=-\infty}^{-1} \alpha E_a(u, p-2u) \\ &\quad - \sum_{u=-\infty}^{+\infty} \sum_{m=-\infty}^{-1} \alpha E_a(u, m-u) \\ &= A_{320}\Delta\sigma_{320} + \sum_{m=0}^{+\infty} \sum_{s=-\infty}^{-2} \alpha E_a(s-2m, 3m-s) \\ &\quad - \sum_{m=-\infty}^{-1} \sum_{s=-1}^{+\infty} \alpha E_a(s-2m, 3m-s) \\ &\quad + \sum_{p=0}^{+\infty} \sum_{s=-\infty}^{-1} \alpha E_a(2p-s, 2s-3p) \\ &\quad - \sum_{p=-\infty}^{-1} \sum_{s=0}^{+\infty} \alpha E_a(2p-s, 2s-3p). \end{aligned} \quad (18)$$

The results for the faces (210), (310) and (320) are

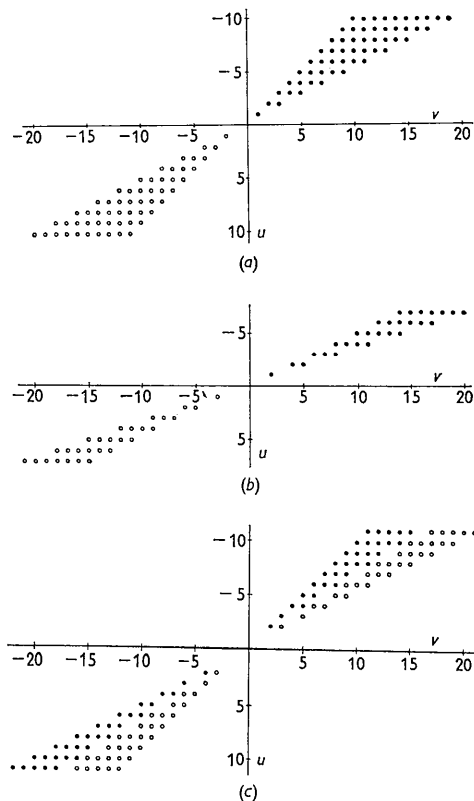


Fig. 3. For each interaction energy $E_a(u, v)$ that enters the expression for $A_{hk0}\Delta\sigma'_{hk0}$ with a positive sign a dot has been placed at the point (u, v) ; for a negative sign an open circle was drawn. (a) shows the (u, v) pairs that enter the expression for (210), (b) those for (310) and (c) those for (320).

visualized in Fig. 3. If for a certain pair of u and v values the interaction energy $E_a(u, v)$ enters the expressions (16), (17) or (18) with a positive sign, a dot has been placed at the point (u.v.); when the sign is negative an open circle is shown.

For non-ionic crystals each $E_a(u, v)$ is negative so that (110) is fairly enhanced; the other S faces are all slightly enhanced. The difference between $\Delta\sigma'_{hko}$ and $\Delta\sigma_{hko}$ becomes smaller with increasing h and k .

Our final conclusion concerning the effect of adsorption on the zonal development of non-ionic crystals is therefore: If adsorption takes place at the step edges only, the face (110) may be fairly enhanced. If adsorption takes place on the whole surface the face (110) may be either enhanced or reduced, depending on the number of occupied adsorption sites per mesh area, but in both cases the effect is slight.

Larger effects are to be expected for ionic crystals.

The interaction energies of ionic chains

Before we proceed to examine the effect of adsorption of ions on the zonal development of ionic crystals, we shall have to find an expression for the interaction energies of ionic chains. In principle this has been done by Madelung (1918) and we shall adapt his formula to the special requirements of our problem.

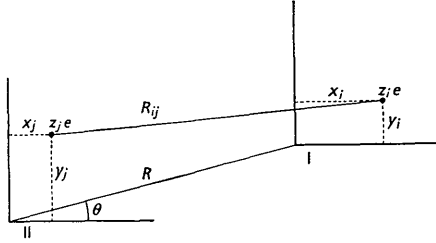


Fig. 4. Coordinates in the interaction energy of two ionic chains. The chains are perpendicular to the plane of drawing.

Consider two chains I and II. The ions of chain I are referred to a Cartesian set of axes; the z -axis is parallel to the chain. The ions of chain II are referred to another Cartesian set of axes which is parallel to the former set. Coordinates of chain I are indicated by the subscript i , those of chain II by the subscript j . See Fig. 4. When the distance between the chains is larger than the period of the chains, the interaction energy is approximated by (cf. Hartman, 1958):

$$E = \Sigma \Sigma -z_i z_j (e^2/p) \ln (R_{ij}^2/4p^2). \quad (19)$$

$z_i e$ and $z_j e$ are the charges of the ions, p is the period of the chain and R_{ij} is the distance between the ions i and j .

According to Fig. 4:

$$R_{ij}^2 = R^2 + 2R(X_i - X_j) \cos \theta + 2R(Y_i - Y_j) \sin \theta + (X_i - X_j)^2 + (Y_i - Y_j)^2.$$

We put:

$$a_{ij} = 2(X_i - X_j) \cos \theta + 2(Y_i - Y_j) \sin \theta$$

$$b_{ij} = (X_i - X_j)^2 + (Y_i - Y_j)^2$$

so that

$$E = \Sigma \Sigma -z_i z_j (e^2/p) [\ln (R^2/4p^2) + \ln (1 + a_{ij}/R + b_{ij}/R^2)].$$

Expansion of the logarithmic function into a series gives:

$$E = \Sigma \Sigma -z_i z_j (e^2/p) [\ln (R^2/4p^2) + A_{ij}R^{-1} + B_{ij}R^{-2} + C_{ij}R^{-3} + D_{ij}R^{-4} + \dots] \quad (20)$$

where:

$$A_{ij} = a_{ij}$$

$$B_{ij} = b_{ij} - a_{ij}^2/2$$

$$C_{ij} = -a_{ij}b_{ij} + a_{ij}^3/3$$

$$D_{ij} = -b_{ij}^2/2 + a_{ij}^2b_{ij} - a_{ij}^4/4.$$

For the interaction of various types of chains we calculate the first coefficient of R^{-n} that differs from zero.

(1) Chain I is electrically neutral: $\Sigma z_i = 0$.

Then:

$$E = K_1 \sin (\theta - \theta_0)/R \quad (21)$$

where

$$K_1 = -2e^2Q_1/p \cos \theta_0 = 2e^2P_1/p \sin \theta_0$$

$$\tan \theta_0 = -P_1/Q_1$$

$$P_1 = \Sigma z_i X_i \Sigma z_j$$

$$Q_1 = \Sigma z_i Y_i \Sigma z_j.$$

(2) Both chains are neutral: $\Sigma z_i = \Sigma z_j = 0$.

Then:

$$E = K_2 \sin 2(\theta - \theta_0)/R^2. \quad (22)$$

where:

$$K_2 = -2e^2Q_2/p \cos 2\theta_0 = 2e^2P_2/p \sin 2\theta_0$$

$$\tan 2\theta_0 = -P_2/Q_2$$

$$P_2 = \Sigma z_i X_i \Sigma z_j X_j - \Sigma z_i Y_i \Sigma z_j Y_j$$

$$Q_2 = \Sigma z_i X_i \Sigma z_j Y_j + \Sigma z_i Y_i \Sigma z_j X_j.$$

When the chains are identical:

$$P_2 = (\Sigma z_i X_i)^2 - (\Sigma z_i Y_i)^2; \quad Q_2 = 2\Sigma z_i X_i \Sigma z_i Y_i.$$

(3) Both chains are neutral, but additional conditions for chain I are:

$$\Sigma z_i X_i = \Sigma z_i Y_i = 0.$$

Then:

$$E = K_3 \sin 3(\theta - \theta_0)/R^3 \quad (23)$$

where:

$$K_3 = 2e^2Q_3/p \cos 3\theta_0 = -2e^2P_3/p \sin 3\theta_0$$

$$\tan 3\theta_0 = -P_3/Q_3$$

$$P_3 = \Sigma z_j X_j (\Sigma z_i X_i^2 - \Sigma z_i Y_i^2) - 2\Sigma z_i X_i Y_i \Sigma z_j Y_j$$

$$Q_3 = \Sigma z_j Y_j (\Sigma z_i X_i^2 - \Sigma z_i Y_i^2) + 2\Sigma z_i X_i Y_i \Sigma z_j X_j.$$

(4) Both chains are neutral, but also

$$\sum z_i X_i = \sum z_i Y_i = \sum z_j X_j = \sum z_j Y_j = 0.$$

Then:

$$E = K_4 \sin 4(\theta - \theta_0)/R^4 \quad (24)$$

where:

$$\begin{aligned} K_4 &= 3e^2 Q_4/p \cos 4\theta_0 = -3e^2 P_4/p \sin 4\theta_0 \\ \tan 4\theta_0 &= -P_4/Q_4 \\ P_4 &= (\sum z_i X_i^2 - \sum z_i Y_i^2)(\sum z_j X_j^2 - \sum z_j Y_j^2) \\ &\quad - 4\sum z_i X_i Y_i \sum z_j X_j Y_j \\ Q_4 &= 2\{\sum z_i X_i Y_i (\sum z_j X_j^2 - \sum z_j Y_j^2) \\ &\quad + \sum z_j X_j Y_j (\sum z_i X_i^2 - \sum z_i Y_i^2)\}. \end{aligned}$$

When the chains are identical:

$$\begin{aligned} P_4 &= (\sum z_i X_i^2 - \sum z_i Y_i^2)^2 - 4(\sum z_i X_i Y_i)^2 \\ Q_4 &= 4\sum z_i X_i Y_i (\sum z_i X_i^2 - \sum z_i Y_i^2). \end{aligned}$$

(5) Conditions for chain I:

$$\sum z_i = 0, \sum z_i X_i = \sum z_i Y_i = 0;$$

for chain II: $\sum z_j \neq 0$.

Then:

$$E = K'_2 \sin 2(\theta - \theta_0)/R^2 \quad (25)$$

$$\begin{aligned} K'_2 &= e^2 G \sum z_j/p \cos 2\theta_0 = -e^2 F \sum z_j/p \sin 2\theta_0 \\ \tan 2\theta_0 &= -F/G \\ F &= \sum z_i X_i^2 - \sum z_i Y_i^2 \\ G &= 2\sum z_i X_i Y_i. \end{aligned}$$

Zonal development of ionic crystals with adsorption

We consider only the case where the adsorption of ions takes place exclusively at the step edges. According to (15) the surface energy per mesh area of (110) changes with a certain amount that involves, among other terms, the interaction energies $E_a(\bar{1}, 0)$ and $E_a(0, \bar{1})$. These energies consist mainly of the bond energy between adsorbed ions and crystal ions in the first coordination sphere, so that the adsorption energy per molecule is of the same order as the crystal energy. Now $\Delta\sigma_{110}$ amounts in general to a few percent of the crystal energy, so that according to (15) the face (110) is much enhanced, even if α is small.

It was shown (Hartman, 1958) that for ionic crystals S faces are not to be expected on equilibrium forms because of the repulsion between the chains. In case of adsorption not only (110), but also other S faces may appear. Which S faces actually appear, depends on the interaction energies between a chain of adsorbed impurity ions and the ionic chains of the crystal. Because these energies depend not only on the distance between the chains, but also on their mutual orientation, it is very well possible that a high index S face becomes more prominent than a low index S face. This high index S face is not necessarily the same for all values of α , the number of adsorbed ions

per mesh area, so that different amounts of adsorbed material produce different zone developments. Yet it often occurs that a face with relatively high indices is observed. Presumably it is even present if the amount of adsorbed material varies within wide limits. The following structural conditions would make this possible:

(1) The face $(hk0)$ ($h > k$) is nearly parallel to a direction in which the interaction energy of the crystal ionic chains is zero; this energy is positive for all faces between $(hk0)$ and (110), negative for faces between $(hk0)$ and (100).

(2) The interaction energy $E_a(u, v)$ is also near to zero in this same direction, but it is positive where the former energy is negative and vice versa.

In this case it is throughout possible that from a certain value of α the $\Delta\sigma'$ values of the faces between (100) and $(hk0)$ become positive, while $\Delta\sigma_{hk0}$ remains negative. The face $(hk0)$ is then always present so that its persistence values may be relatively high, and the zone development does not conform to the law of Donnay & Harker (1937). The anomalous development will be discussed in the following examples.

Examples

(1) *Zircon*, $[\bar{1}11]$ zone

In Table 1 the faces between (101) and (110) are arranged according to increasing mesh areas. The

Table 1. *Persistences of faces in the zone $[\bar{1}11]$ of zircon*

Face	P	F	New indices	Angle with (110)
110	58	75	100	0° 00'
101	88	96	010	61° 40'
211	58	65	110	31° 43'
321	12	10	210	20° 21'
312	—	—	120	42° 50'
431	—	—	310	14° 50'
413	—	—	130	48° 03'
532	12	6	320	24° 51'

persistence values (Hartman, 1956) should decrease in the same order if the zone were normally developed. The persistence of (532) is much higher than would be expected. To find out the peculiar structural position of this face we consider a projection of the structure along $[\bar{1}11]$ (Fig. 5). Each silicate SiO_4^{4-} ion is represented by one circle and in the calculations the zircon and silicate ions are considered as point charges. The whole structure can be divided into a set of neutral chains parallel to $[\bar{1}11]$. These chains are closest together in directions parallel to (110) and (101). For the application of the formulas derived in the foregoing sections it is convenient to give new indices. The faces (110), (101) and (211) are given the new indices (100), (010) and (110), respectively (cf. Table 1); the face (532) becomes (320).

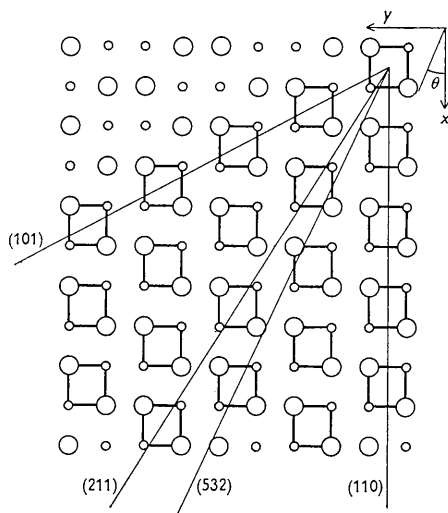


Fig. 5. Projection of the zircon structure parallel to $[\bar{1}11]$. Large circles: SiO_4 ; small circles: Zr. Ions belonging to one chain are connected. The directions of some faces are drawn.

To calculate $\Delta\sigma_{hko}$ we need the interaction energies $E(u, v)$ of the chains. When the X and Y axes are chosen as indicated in the figure, we find that $\sum z_i X_i = \sum z_i Y_i = 0$, so that (24) applies. Then $Q_4 = 0$, $P_4 = -4a^4c^2/(2a^2+c^2)$, $\theta_0 = 22^\circ 30'$ and $E(u, v) = 3e^2P_4 \cos 4\theta/pR^4$, where $p = \frac{1}{2}\sqrt{(2a^2+c^2)}$.

This result is also obtained when the oxygen atoms are taken into account and when it is assumed that they are tetrahedrally arranged round the Si-atom.

The energies $E(u, v)$ were calculated for values of u from 1 to 15 and of v from $\bar{1}$ to $\bar{17}$. For various faces $\Delta\sigma_{hko}$ becomes according to (2):

$$\begin{aligned}\Delta\sigma_{110} &= 1.206e^2a^{-3} \\ \Delta\sigma_{120} &= 0.283e^2a^{-3} \\ \Delta\sigma_{210} &= -0.086e^2a^{-3} \\ \Delta\sigma_{310} &= -0.047e^2a^{-3} \\ \Delta\sigma_{320} &= 0.004e^2a^{-3}.\end{aligned}$$

Because of the high positive value of $\Delta\sigma_{110}$, neither (110) nor any other face between (100) and (010) is present on the equilibrium form. When the surface energies are sufficiently lowered by adsorption, the face (110) appears. $\Delta\sigma_{120}$ is fairly positive compared with $\Delta\sigma_{210}$, so that it is to be expected that (210) is easier produced than (120). This agrees well with the higher persistence value of (210). We note that $\Delta\sigma_{320}$ is close to zero. The function $E(u, v)$ is zero for $\theta = 22^\circ 30'$ and (320) corresponds to a value of $\theta = 24^\circ 51'$.

It will be shown now that it is possible to find a configuration of adsorbed ions that produces (320). Suppose that a positive and a negative ion are adsorbed at the step edges in such a way that $\sum z_j X_j = 0$, while $\sum z_j Y_j = zg$, z being the charge of the positive ion. The interaction energy of these ions with the crystal

ionic chains is given by (23). In the present case $Q_3 = 0$, $P_3 = -2a^2czg(2a^2+c^2)^{-\frac{1}{2}}$, $\theta_0 = 30^\circ$ and $E(u, v) = 2e^2P_3 \cos 3\theta/pR^3$. These energies were calculated for values of u from 1 to 12 and of v from $\bar{1}$ to $\bar{12}$. Applying (16), (17) and (18), we find:

$$\begin{aligned}\Delta\sigma'_{210} &= (-0.086 + 0.068\beta)e^2a^{-3} \\ \Delta\sigma'_{310} &= (-0.047 + 0.143\beta)e^2a^{-3} \\ \Delta\sigma'_{320} &= (0.004 - 0.014\beta)e^2a^{-3}.\end{aligned}$$

Here $\beta = \alpha zg/a$. These relations are graphically represented in Fig. 6. As (310) is very rare, we might

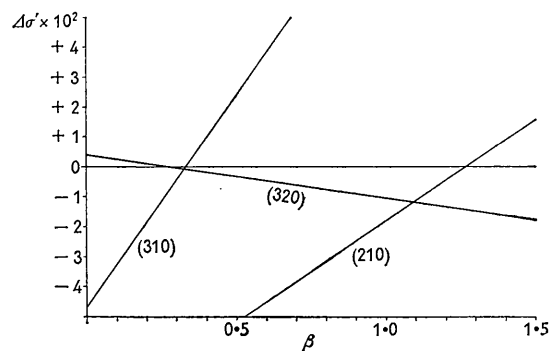


Fig. 6. Graph of $\Delta\sigma'$ versus β for various faces of zircon.

suppose that in practice β ranges between 0.3 and 1.4. Within this range (210) and (320) may appear. For $\beta = 0.35$ (210) is relatively large while (320) is very narrow. With increasing β the breadth of (210) decreases, while that of (320) increases until at about $\beta = 1.0$ (210) is entirely obliterated by (320). This last effect cannot be read off from Fig. 6, but it follows from a calculation of the breadth:

$$b_{210} = \Delta\sigma'_{210} \{ \cot (100):(210) + \cot (110):(210) \} - \Delta\sigma'_{320} \operatorname{cosec} (210):(320).$$

Thus we see that the adsorption of impurity ions for a wide range of concentrations can account for the appearance of (210) and (320), while (310) is absent. The adsorption sites may be those of the Zr and SiO_4 ions, when $g = \frac{1}{4}a/2$. With $z = 4$, the maximum value of β is $\sqrt{2}$.

Table 2. *Persistences of faces in the zone [100] of anatase*

Face	P	F	New indices	Angle with (001)
001	50.0	65.0	100	$0^\circ 00'$
011	81.2	98.5	010	$68^\circ 18'$
013	31.5	22.5	110	$39^\circ 57'$
015	17.6	18.5	210	$26^\circ 41'$
012	14.5	18.0	120	$51^\circ 29'$
017	36.5	27.5	310	$19^\circ 45'$
035	14.5	3.0	130	$56^\circ 27'$
019	4.4	1.5	410	$15^\circ 36'$
014	5.7	4.5	320	$32^\circ 08'$
037	3.1	7.5	230	$47^\circ 07'$

(2) *Anatase*, [100] zone

The faces of the [100] zone between (001) and (011) have been listed in Table 2 according to increasing mesh areas. The persistence values (Parker, 1923) should decrease in the same order. Apart from (011), (017) has persistence values not in accordance with its rank. Fig. 7 gives a projection of the anatase

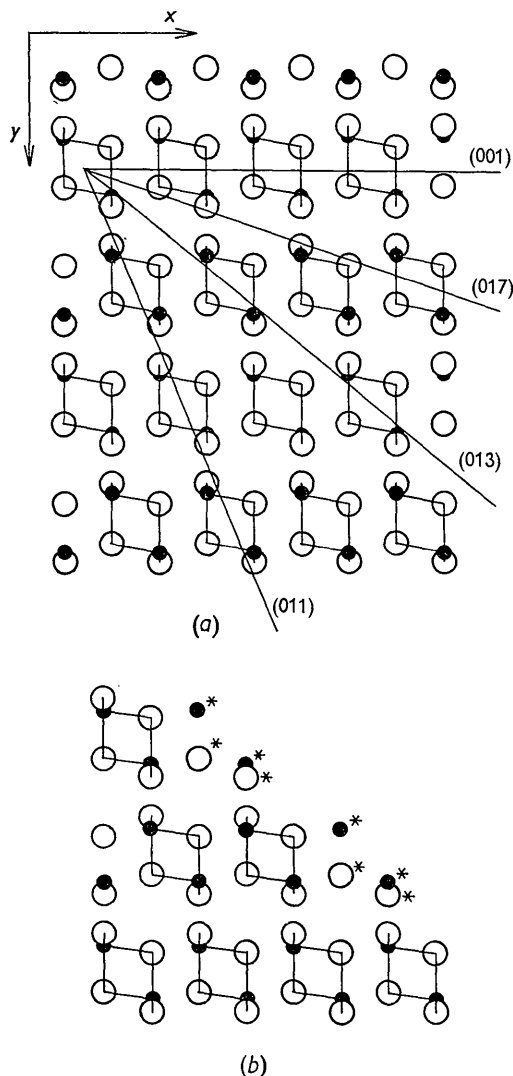


Fig. 7. Projection of the anatase structure parallel to [100]. Open circles: O; closed circles: Ti. Ions belonging to one chain are connected. (a) Directions of some faces are shown. (b) Profile of (013) with adsorbed ions, indicated with asterisks, in crystal ion sites.

structure on (100) in which chains parallel to [100] and of composition Ti_2O_4 are indicated. As the chains consist of uninterrupted strong bonds, they are periodic bond chains. These chains are closest together in the directions of the faces (011) and (001), where they are linked to each other by strong Ti-O bonds. The faces (001) and (011) are therefore *F* faces. For the calcula-

tion of the chain interaction energies it is convenient to take new indices: the faces (001), (011) and (013) are given the indices (100), (010) and (110), respectively (see Table 2). The chain interaction energies are again calculated with (24): the *X* and *Y* axes have been indicated in Fig. 7. The parameter *u* of the O atom in $(0, 0, u)$ is put equal to $\frac{5}{24}$; the axial ratio $c/a = 2.5133$. Then $\sum z_i X_i^2 = 0$, $\sum z_i Y_i^2 = -c^2/72$, $\sum z_i X_i Y_i = \frac{1}{6}ac$, from which $\theta_0 = 19^\circ 31'$. The interaction energies $E(u, v)$ were calculated for *u* ranging from $\bar{1}$ to $\bar{12}$ and for *v* ranging from 1 to 18. The correction terms of the surface energies, $\Delta\sigma_{hko}$, were calculated according to (2). We find:

$$\begin{aligned}\Delta\sigma_{110} &= 0.1264e^2a^{-3} \\ \Delta\sigma_{210} &= 0.0086e^2a^{-3} \\ \Delta\sigma_{310} &= -0.0012e^2a^{-3} \\ \Delta\sigma_{410} &= -0.0011e^2a^{-3} \\ \Delta\sigma_{510} &= -0.0006e^2a^{-3} \\ \Delta\sigma_{120} &= 0.0100e^2a^{-3}.\end{aligned}$$

Just as in the case of zircon, no *S* faces are present on the equilibrium form, because of the high positive value of $\Delta\sigma_{110}$. We note that (310) is parallel to the direction $\theta = 19^\circ 45'$, while the function $E(u, v)$ is zero for $\theta = 19^\circ 31'$.

The values $\Delta\sigma_{210}$ and $\Delta\sigma_{120}$ are of the same order of magnitude; this agrees well with the persistences, which are also about the same. The $\Delta\sigma$ values of (310), (410) and (510) are negative. As a consequence these faces may well appear before (210) when the surface energy is lowered by adsorption. A calculation shows that if impurity ions A^+ and B^- are placed at a step edge in the sites of the Ti and O atoms indicated with an asterisk in Fig. 7(b), (510) is actually produced before (410), (310) and (210). With increasing impurity concentration (410) appears; then (210) appears while (510) disappears, until at last (310) appears. With still higher concentrations (410) disappears first, followed by (310), so that (210) remains. From these processes it may be inferred that an anomalous zone development is certainly possible. The calculations and the parameter *u* are too uncertain, however, to allow definite conclusions as to the expected persistence values. Variation of a few per cent in the parameter *u* would be sufficient to make (310) persist without (510), (410) and (210) for a certain range of adsorbed impurity concentrations, which would account for the relatively high persistences of this face.

(3) *Fluorite*

According to the statistical investigations of Holzgang (1930) the ten most important fluorite forms are: {001}, {111}, {011}, {113}, {013}, {124}, {112}, {012}, {137} and {3,5,11}. Seven out of these forms lie on the zone $[11\bar{2}]$. Faces between $(\bar{1}10)$ and (111) have been arranged in Table 3 according to increasing mesh areas. If we compare this order with the persistence

Table 3. Persistence values of faces in the zone $[11\bar{2}]$ of fluorite

Face	P	Angle with (110)	New indices
111	44.8	90° 00'	010
$\bar{1}10$	38.1	0° 00'	100
$\bar{1}31$	16.0	31° 29'	110
021	8.7	50° 46'	120
$\bar{3}51$	0.3	17° 01'	210
153		61° 26'	130
132	3.3	67° 48'	140
$\bar{1}73$	7.3	42° 34'	230
$\bar{5}71$	0.3	11° 32'	310
375	0.0	71° 55'	150
$\bar{2}41$	12.2	22° 12'	320
195	0.0	56° 51'	250
243	0.0	74° 47'	160
$\bar{1}52$	0.1	39° 13'	340
$\bar{7}91$	0.0	8° 42'	410
$\bar{1},11,5$	0.0	45° 35'	350
$\bar{5},11,3$	5.5	24° 40'	430
597	0.0	76° 52'	170

values found by Holzgang (1930), we see that four faces have an abnormally high P value, namely ($\bar{2}41$), ($\bar{1}73$), ($\bar{5},11,3$) and (132). Fig. 8 gives a projection of the fluorite structure parallel to $[11\bar{2}]$. Along this direction the structure has ionic chains of composition CaF_2 . This chain does not consist of an uninterrupted series of strong bonds, so that it is no P.B.C. Most of the faces are K faces. The results of the foregoing sections are applicable to all kinds of zones, when the most densely packed faces are considered as the new

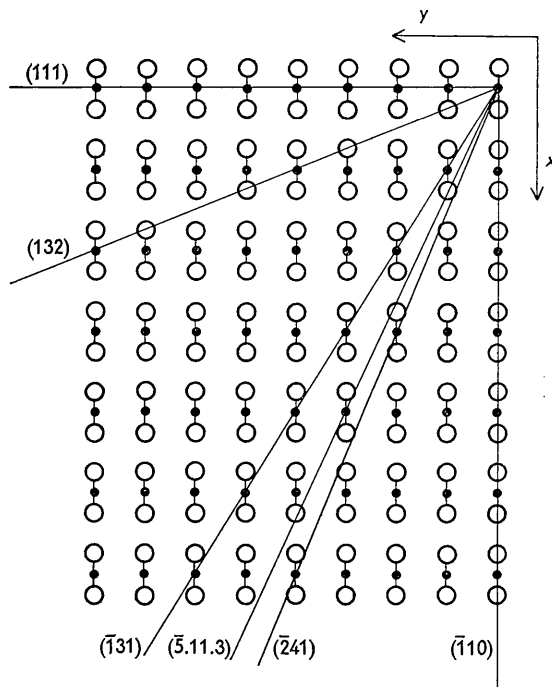


Fig. 8. Projection of the fluorite structure parallel to $[11\bar{2}]$. Open circles: F; closed circles: Ca. Ions belonging to one chain are connected.

(100) and (010) faces. In the present case these are the faces ($\bar{1}10$) and (111).

To calculate the interaction energy between the chains, the X and Y axes are taken as indicated in Fig. 8. Then $\sum z_i X_i^2 < 0$, $\sum z_i Y_i^2 = 0$ and $\sum z_i X_i Y_i = 0$, from which $\theta_0 = 22^\circ 30' \pm n. 45^\circ$. The energy $E(\bar{1}, 1)$ as calculated by (24) is negative, which would imply that ($\bar{1}31$) is present when (111) and ($\bar{1}10$) are present. However, for short distances between the chains the approximation (19) does not hold, since the period of the chain $[\frac{1}{2}, \frac{1}{2}, \bar{1}]$ is rather long. The exact value of $E(\bar{1}, 1)$ appears to be positive, so that ($\bar{1}31$) is present only when foreign ions are adsorbed on it.

We note that the faces ($\bar{2}41$) and ($\bar{5},11,3$) are nearly parallel to the direction $\theta_0 = 22^\circ 30'$, while (132) is nearly parallel to $\theta_0 = 67^\circ 30'$.

The surface of the fourth anomalous face ($\bar{1}73$) is not parallel to a direction in which the chain interaction energy is zero, but in the zone $[301]$ it is. Let us consider the symmetrically equivalent zone $[3\bar{1}0]$.

Table 4. Persistences of faces in the zone $[3\bar{1}0]$ of fluorite

Face	P	Angle with (001)	New indices
001	81.8	0° 00'	100
131	16.0	72° 27'	010
133	4.2	46° 30'	110
135	0.3	32° 19'	210
132	3.3	57° 41'	120
137	7.3	24° 18'	310
139	1.4	19° 21'	410
134	0.6	38° 20'	320

In Table 4 the faces have been arranged again ac-

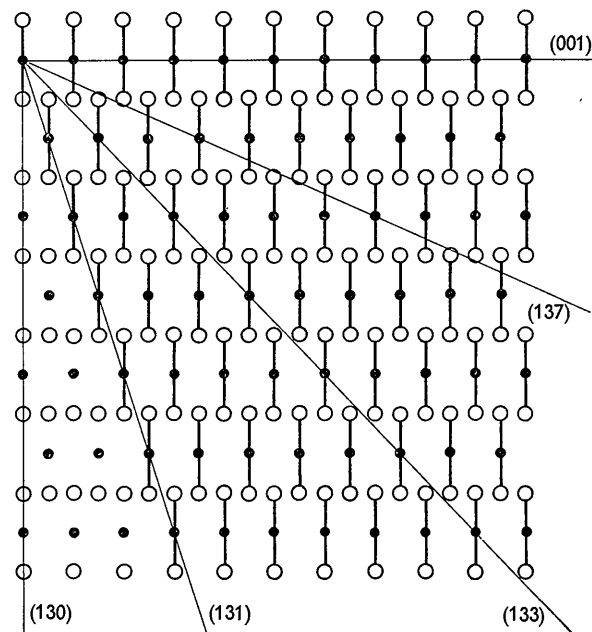


Fig. 9. Projection of the fluorite structure parallel to $[3\bar{1}0]$. Open circles: F; closed circles: Ca. Ions belonging to one chain are connected.

ording to increasing mesh areas. Fig. 9 gives a projection of the structure along $[3\bar{1}0]$. The CaF_2 chains in this projection have the same structure as in the $[11\bar{2}]$ projection: centrosymmetrical about the Ca ion and all ions lying in one plane. The interaction energy between these chains is zero in the directions that make angles of $22^\circ 30'$ or of $67^\circ 30'$ with (001). From Table 4 we see that indeed (137) includes an angle close to $22^\circ 30'$ with (001).

(4) Anatase, $[35\bar{1}]$ zone

We return to anatase where the form $\{3,2,19\}$ has the rather high persistence of 15.7 (Parker, 1923). The smallest translation period in the face (3,2,19) is $[\frac{3}{2}, \frac{2}{19}, \frac{1}{2}]$. Fig. 10 gives a projection of the structure

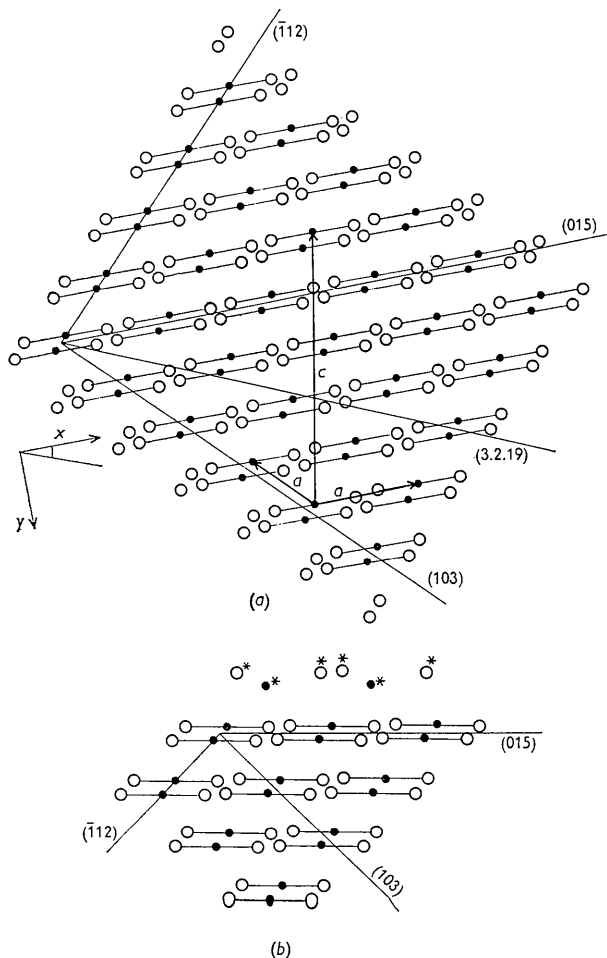


Fig. 10. Projection of the anatase structure parallel to $[35\bar{1}]$. Open circles: O; closed circles: Ti. Ions belonging to one chain of composition TiO_2 are connected. The primitive cell of the projection contains two of such chains close together. (a) The axes of the conventional body centred unit cell are shown. (b) Profile of (015) with adsorbed ions in the sites of crystal ions, indicated with asterisks.

parallel to this direction. The most densely packed faces in this zone are (103) and $(\bar{1}12)$. Faces between

Table 5. Persistences of faces in the zone $[35\bar{1}]$ of anatase

Face	P	Angle with the plane of the chains	New indices
103	31.5	$43^\circ 41'$	100
$\bar{1}12$	48.4	$-47^\circ 27'$	010
015	17.6	$-3^\circ 05'$	110
118	1.9	$15^\circ 56'$	210
$\bar{1}27$	0.0	$-21^\circ 36'$	120
2,1,11	0.0	$24^\circ 25'$	310
$\bar{2}39$	0.0	$-29^\circ 36'$	130
1,2,13	0.6	$8^\circ 32'$	320
$\bar{1},3,12$	0.0	$-14^\circ 31'$	230
3,1,14	0.0	$29^\circ 01'$	410
$\bar{3},4,11$	0.0	$-33^\circ 54'$	140
1,3,18	0.0	$5^\circ 15'$	430
$\bar{1},4,17$	0.0	$-11^\circ 19'$	340
4,1,17	0.0	$31^\circ 52'$	510
4,5,13	0.0	$-36^\circ 33'$	150
3,2,19	15.7	$20^\circ 54'$	520
3,5,16	0.0	$-26^\circ 18'$	250

these two faces are listed according to increasing mesh areas in Table 5. In this sequence the face (3,2,19) occupies the 16th rank. From the 5th rank on all faces have a P value of 0.6 or smaller (Parker, 1923). Parallel to the zone $[35\bar{1}]$ we find chains of composition TiO_2 ; two of such chains occur in the primitive unit cell. The chains have the same centrosymmetrical structure as those encountered in fluorite. In the projection the two O ions and the central Ti ion lie on a straight line, which is taken as X axis. The directions of zero chain interaction energy lie at angles of $22^\circ 30'$ and of $67^\circ 30'$ with this line. The surface of (3,2,19) corresponds with $\theta = 20^\circ 54'$.

According to Table 5 other faces also are near to a direction of zero chain interaction energy. When (103), $(\bar{1}12)$ and (015) are given the new indices (100), (010) and (110), respectively, these faces are (120) and (310). Because of their smaller mesh areas they might be expected to be more persistent than (520). In fact they are not and this must be caused by the special nature of the adsorption. The foreign ions are likely to be located nearly in the sites of the crystal ions. The chains of adsorbed ions are very likely to be neutral, so that the interaction energy with the crystal ionic chains is given by (23). From the fact that (520) has a higher persistence than (310) we infer that $\Delta\sigma'_{520}$ is negative, while $\Delta\sigma'_{310}$ is positive. Now, if we take into account that according to (23) $E_a(\bar{u}, v) = -E_a(u, \bar{v})$, we find from (17):

$$A_{310}\Delta\sigma'_{310} = A_{310}\Delta\sigma_{310} + \alpha[E_a(\bar{1}, 2) + E_a(\bar{1}, 3) + E_a(\bar{2}, 4) + 2E_a(\bar{2}, 5) + E_a(\bar{2}, 6) + E_a(\bar{3}, 6) + 2E_a(\bar{3}, 7) + 2E_a(\bar{3}, 8) + E_a(\bar{3}, 9) + \dots].$$

Similarly:

$$A_{520}\Delta\sigma'_{520} = A_{520}\Delta\sigma_{520} + \alpha[E_a(\bar{2}, 4) + E_a(\bar{2}, 6) + E_a(\bar{3}, 6) - E_a(\bar{3}, 7) - E_a(\bar{3}, 8) - E_a(\bar{3}, 9) \dots].$$

$A_{310}\Delta\sigma_{310} \approx E(\bar{1}, 3)$ is slightly negative and $A_{520}\Delta\sigma_{520} \approx E(\bar{2}, 5)$ is slightly positive. $\Delta\sigma_{310}$ can become positive, and $\Delta\sigma_{520}$ negative, if $E_a(\bar{2}, 5)$, $E_a(\bar{3}, 7)$ and $E_a(\bar{3}, 8)$ are positive, while $E_a(\bar{1}, 2)$ is nearly zero, or even slightly positive. Let us assume that $E_a(\bar{1}, 2) = 0$, so that $\theta_0 = 15^\circ 56'$. In that case according to (23), $P_3/Q_3 = -\tan 47^\circ 48'$ and, since $\Sigma z_i Y_i^2 = \Sigma z_i X_i Y_i = 0$, we find that $\Sigma z_j Y_j / \Sigma z_j X_j = -\tan 42^\circ 12'$.

For the three ions A^{++} , B^- and C^- located in the sites of Ti and O atoms (see Fig. 10(b)), we find $\Sigma z_j Y_j / \Sigma z_j X_j = -\tan 47^\circ 27'$, the line joining the centre of gravity of the negative ions with the positive ion being parallel to (010). The interaction energy of these adsorbed ions with the crystal ionic chains becomes zero for $\theta = 14^\circ 11'$. $E_a(\bar{1}, 2)$ is slightly positive, so that these adsorbed ions fulfill the requirements for the appearance of (520).

For the face (120) to appear, $\Delta\sigma'_{120}$ should be slightly negative and $\Delta\sigma'_{130}$ should be positive. A combination of adsorbed ions in sites of crystal ions that would produce this face, could not be found.

(5) Conclusions

Up to now the appearance of crystal faces with high indices (not vicinal faces) could not be explained. The examples seem to reveal at least one of their special properties: they are all parallel (within 3°) to a

direction in which the interaction energy of the crystal ionic chains is zero. For zircon and anatase it was shown that adsorption of foreign ions might produce high index faces on the equilibrium form which are not exhibited without adsorption and the appearance of which violates the law of Donnay & Harker (1937). The foreign ions were assumed to be located in sites which, if growth would proceed were to be occupied by crystal ions.

In choosing the examples among the minerals, two assumptions were made. First, that the calculations, although strictly valid at 0°K ., apply also at other temperatures. Second, that the crystals found in nature represent approximately equilibrium forms. The results obtained seem to justify these assumptions.

The author is indebted to Dr W. G. Perdok for discussions and advice.

References

- DONNAY, J. D. H. & HARKER, D. (1937). *Amer. Min.* **22**, 446.
 HARTMAN, P. (1956). *Acta Cryst.* **9**, 721.
 HARTMAN, P. (1958). *Acta Cryst.* **11**, 459.
 HOLZGANG, F. (1930). *Schweiz. Min. und Petr. Mitt.* **10**, 374.
 MADELUNG, E. (1918). *Phys. Z.* **19**, 524.
 PARKER, R. L. (1923). *Z. Kristallogr.* **58**, 522.

Acta Cryst. (1959). **12**, 439

On the Fourier Treatment of Distortion Broadening in X-ray Diffraction

BY JON GJØNNES

Central Institute for Industrial Research, Oslo, Norway

(Received 24 November 1958)

General expressions for the Patterson function and intensity distribution in reciprocal space of a distorted crystal are derived. It is shown that the intensity distributions of the broadened reflexions are given as sections through the six-dimensional Fourier transform of a strain distribution function. Relationship with earlier work and application to one-dimensional intensity distributions, such as powder diffractograms, are discussed.

1. Introduction

The effect of lattice distortions upon the distribution of diffracted X-ray intensity has been treated by several authors (Stokes & Wilson, 1944; Warren & Averbach, 1950; Warren, 1955) and methods have been devised to evaluate lattice strains from X-ray measurements in the case of small distortions (Warren & Averbach, 1950, 1952). It is the purpose of this paper to point out that a general description of lattice distortions may be given in reciprocal space as well as in physical space by introducing the (six-dimensional) Fourier transform $\psi(\mathbf{t}; \mathbf{s})$ of the distribution function

$W(\mathbf{r}; \mathcal{E})$ for integral strain \mathcal{E} over distances \mathbf{r} . This function $\psi(\mathbf{t}; \mathbf{s})$ includes both the exact line profiles and the approximate expressions used in the references. The representation offered may thus be employed to investigate the significance of these approximations and eventually as a basis for more exact methods.

2. Intensity distribution in reciprocal space

As a starting point of our discussion, let us review the derivation of the intensity distribution for a distorted crystal. We prefer to use the 'continuous representation': Let the positions \mathbf{p} of the elements of volume